### RAPID COMMUNICATION



# Recurrent acute liver failure due to NBAS deficiency: phenotypic spectrum, disease mechanisms, and therapeutic concepts

Christian Staufner  $^1$  · Tobias B. Haack  $^{2,3}$  · Marlies G. Köpke  $^3$  · Beate K. Straub  $^4$  · Stefan Kölker  $^1$  · Christian Thiel  $^1$  · Peter Freisinger  $^5$  · Ivo Baric  $^6$  · Patrick J. McKiernan  $^7$  · Nicola Dikow  $^8$  · Inga Harting  $^9$  · Flemming Beisse  $^{10}$  · Peter Burgard  $^1$  · Urania Kotzaeridou  $^1$  · Dominic Lenz  $^1$  · Joachim Kühr  $^{11}$  · Urban Himbert  $^{12}$  · Robert W. Taylor  $^{13}$  · Felix Distelmaier  $^{14}$  · Jerry Vockley  $^{15}$  · Lina Ghaloul-Gonzalez  $^{15}$  · John A. Ozolek  $^{16}$  · Johannes Zschocke  $^{17}$  · Alice Kuster  $^{18}$  · Anke Dick  $^{19}$  · Anib M. Das  $^{20}$  · Thomas Wieland  $^3$  · Caterina Terrile  $^3$  · Tim M. Strom  $^{2,3}$  · Thomas Meitinger  $^{2,3}$  · Holger Prokisch  $^{2,3}$  · Georg F. Hoffmann  $^1$ 

Received: 28 July 2015 / Accepted: 28 September 2015 © SSIEM 2015

#### Abstract

Background Acute liver failure (ALF) in infancy and child-hood is a life-threatening emergency and in about 50 % the etiology remains unknown. Recently biallelic mutations in NBAS were identified as a new molecular cause of ALF with

onset in infancy, leading to recurrent acute liver failure (RALF).

*Methods* The phenotype and medical history of 14 individuals with NBAS deficiency was studied in detail and functional studies were performed on patients' fibroblasts.

Communicated by: Bruce A Barshop

Christian Staufner, Tobias B. Haack, Holger Prokisch and Georg F. Hoffmann contributed equally to this work.

**Electronic supplementary material** The online version of this article (doi:10.1007/s10545-015-9896-7) contains supplementary material, which is available to authorized users.

- Georg F. Hoffmann georg.hoffmann@med.uni-heidelberg.de
- Department of General Pediatrics, Division of Neuropediatrics and Pediatric Metabolic Medicine, University Hospital Heidelberg, 69120 Heidelberg, Germany
- Institute of Human Genetics, Technische Universität München, 81675 Munich, Germany
- <sup>3</sup> Institute of Human Genetics, Helmholtz Zentrum München, 85764 Neuherberg, Germany
- Institute of Pathology, University Hospital Heidelberg, 69120 Heidelberg, Germany
- <sup>5</sup> Children's Hospital Reutlingen, 72764 Reutlingen, Germany
- Department of Pediatrics, University Hospital Center Zagreb and University of Zagreb, School of Medicine, 10000 Zagreb, Croatia
- Liver Unit, Birmingham Children's Hospital, Birmingham B4 6NH, UK

Published online: 05 November 2015

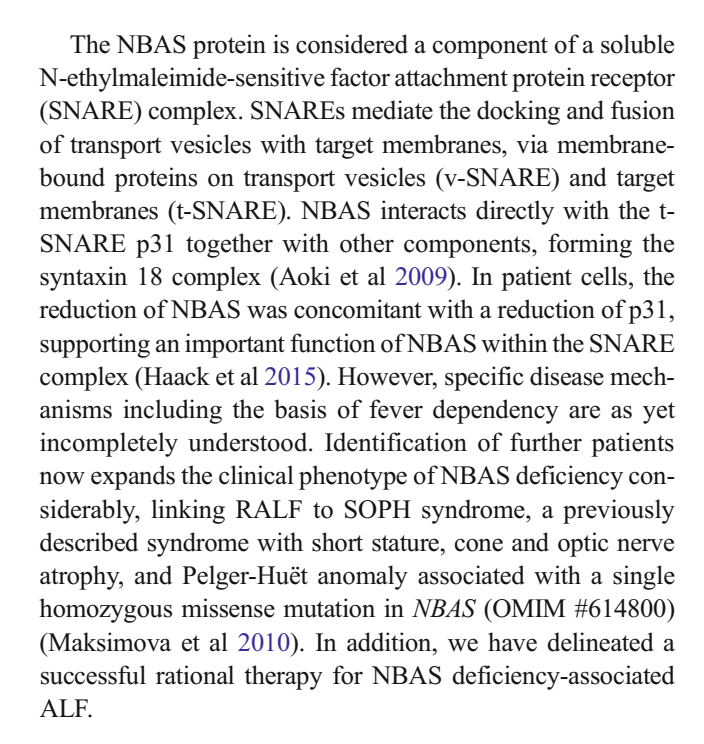
- Institute of Human Genetics, University Hospital Heidelberg, 69120 Heidelberg, Germany
- Department of Neuroradiology, University Hospital Heidelberg, 69120 Heidelberg, Germany
- Ophthalmology Department, University Hospital Heidelberg, 69120 Heidelberg, Germany
- Children's Hospital Karlsruhe, 76133 Karlsruhe, Germany
- <sup>12</sup> Children's Hospital St. Elisabeth, 56564 Neuwied, Germany
- Wellcome Trust Centre for Mitochondrial Research, Institute of Neuroscience, The Medical School, Newcastle University, Newcastle upon Tyne NE2 4HH, UK
- Department of General Pediatrics, Neonatology and Pediatric Cardiology, University Children's Hospital, Heinrich-Heine-University Düsseldorf, 40225 Duesseldorf, Germany
- University of Pittsburgh School of Medicine, Children's Hospital of Pittsburgh of UPMC, Pittsburgh, PA 15224, USA



Results The phenotypic spectrum of NBAS deficiency ranges from isolated RALF to a multisystemic disease with short stature, skeletal dysplasia, immunological abnormalities, optic atrophy, and normal motor and cognitive development resembling SOPH syndrome. Liver crises are triggered by febrile infections; they become less frequent with age but are not restricted to childhood. Complete recovery is typical, but ALF crises can be fatal. Antipyretic therapy and induction of anabolism including glucose and parenteral lipids effectively ameliorates the course of liver crises. Patients' fibroblasts showed an increased sensitivity to high temperature at protein and functional level and a disturbed tethering of vesicles, pointing at a defect of intracellular transport between the endoplasmic reticulum and Golgi.

Conclusions Mutations in NBAS cause a complex disease with a wide clinical spectrum ranging from isolated RALF to a multisystemic phenotype. Thermal susceptibility of the syntaxin 18 complex is the basis of fever dependency of ALF episodes. NBAS deficiency is the first disease related to a primary defect of retrograde transport. Identification of NBAS deficiency allows optimized therapy of liver crises and even prevention of further episodes.

In about 50 % of cases with acute liver failure (ALF) in infancy and childhood the etiology remains unresolved (Squires et al 2006, Narkewicz et al 2009). Unknown diagnosis significantly hampers decision-making on appropriate treatment strategies up to allocation to liver transplantation. Inborn errors of metabolism comprise one of the most frequently detected groups of diseases causing pediatric ALF. These include mitochondrial diseases, Wilson disease, tyrosinemia type I, fatty acid oxidation defects, urea cycle disorders, citrin deficiency, galactosemia, hereditary fructose intolerance, and Niemann-Pick type C (Squires et al 2006, Narkewicz et al 2009). It has been speculated that a significant number of individuals with indeterminate ALF are due to as yet unknown metabolic disorders or atypical clinical presentations of known metabolic disorders (Vilarinho et al 2014). Recently we have identified biallelic mutations in neuroblastoma amplified sequence (NBAS) as a novel cause of ALF with onset infancy (Haack et al 2015). Given 14 patients have been identified within a reasonably short time frame, defects in this gene appear to be a relatively frequent cause of pediatric ALF.



### **Methods**

#### **Patients**

We studied in detail the phenotypic spectrum of 14 patients from 13 families with (recurrent) ALF and biallelic mutations in *NBAS* by a prospective observational follow-up study and by thoroughly evaluating the medical history. ALF was defined as an international normalized ratio (INR) above 2 or INR above 1.5 and encephalopathy grade III or IV according to the definition of the PALF study group (Squires et al 2006). Informed consent to participate in the study was obtained from all patients or their parents in case of minor patients.

The study was approved by the ethical committee of the University Hospital Heidelberg (S-035/2014). The identification of the genetic defect and a brief clinical description of patients 1–11 has been published recently (Haack et al 2015). Patient 11 was originally diagnosed as having ACAD9 deficiency on the basis of abnormal immunostaining and RNA processing studies (He et al 2007); however, genomic



Department of Pathology, Children's Hospital of Pittsburgh of UPMC, University of Pittsburgh School of Medicine, Pittsburgh, PA 15224, USA

Division of Human Genetics, Innsbruck Medical University, 6020 Innsbruck, Austria

<sup>&</sup>lt;sup>18</sup> Inborn Errors of Metabolism, Pediatric Intensive Care Unit, University Hospital of Nantes, 44093 Nantes, France

Department of Pediatrics, University Hospital Würzburg, 97080 Wuerzburg, Germany

Clinic for Pediatric Kidney-, Liver- and Metabolic Diseases, Hannover Medical School, 30625 Hannover, Germany

mutations in *ACAD9* were not found. Patients 12, 13, and 14 have been diagnosed by exome sequencing as described previously (Haack et al 2012). In patients 12 and 13 copy number variants calling using ExomDepth indicated heterozygous deletions of coding exons 49–50 and 39–40, respectively, in addition to heterozygous point mutations predicting the change of an evolutionarily highly conserved amino acid residue (c.1278A>C, p.Cys426Trp, patient 13) or premature truncation of the protein (c.2827G>T, p.Glu943\*, patient 12).

# Microscopy of fibroblasts and liver

For hematoxylin and eosin staining as well as immunohistochemistry, liver biopsies were routinely fixed in formaldehyde and embedded in paraffin. Immunohistochemistry and immunofluorescence microscopy was performed as previously described (Straub et al 2008: Pawella et al 2014). For ultrastructural analysis, biopsies were fixed in glutaraldehyde and embedded in epon or processed from paraffin blocks to epon. Thin sections were analyzed in a transmission electron microscope (JEM 1400, JEOL). Mouse monoclonal antibodies were against the ER proteins PDI (protein disulfide isomerase; 1D3, Enzo Life Sciences), Bap31 (7A3BB6), epoxide hydrolase (both abcam, Cambridge, UK), the Golgi protein GM130 (abcam), CHOP (9C8, Thermo Scientific/Pierce), and the lipid droplet-associated protein perilipin 2 (AP 125; Progen Heidelberg); additionally, rabbit antisera were used against NBAS (Atlas Antibodies). Concerning secondary antibodies see references (Straub et al 2008; Pawella et al 2014).

### Ex vivo studies in patient and control fibroblasts

Western blot and growth rate detection

Patient and control fibroblasts were cultivated in D-MEM supplemented with 10 % FBS, 1 % Penicillin-Streptomycin, and 200 µM uridine at 37 and 40 °C, respectively, and 5 % CO<sub>2</sub>. For western blots, cells were collected, washed in PBS, and resolved in RIPA buffer. For every sample 10 µg of protein were separated on a 4-12 % acrylamide gradient gel (LONZA). Primary antibodies (all Sigma-Aldrich; all diluted in 5 % milk) against NBAS (1:2000), p31 (USE-1) (1:250) and β-actin (1:15,000), were incubated overnight. Enhanced chemiluminescence of proteins was detected using a Vilberscan Fusion FX7. Protein levels were quantified using the software Bio-1D. For growth curves, patient and control fibroblasts were cultivated on 24-well plates; 2500 cells (determined with a Scepter<sup>TM</sup> cell counter, Millipore) were plated per well and cell growth was assessed by quantification of DNA (CyQUANT®, Molecular Probes) according to the manufacturer's protocol. Cell number was calculated based on a standard curve ( $R^2$ =0.996).

Permeabilization of patient-derived fibroblasts with digitonin and immunofluorescence microscopy

Digitonin permeabilization (Aoki et al 2009) and immunofluorescence staining were performed as described previously (Lubbehusen et al 2010). Digitonin exposure time was 15 min. To induce further NBAS depletion, fibroblasts were incubated at 40 °C for 24 h prior to the experiment. Primary antibodies against ERGIC53 (rabbit against human) and GOLPH4/GPP130 (mouse against human) were purchased from Alexis/Enzo Life Science (Lörrach, Germany) and Abnova (Paderborn, Germany), respectively, and used in a dilution of 1:400 in 1 % BSA (diluted with PBS). Primary antibodies against KDEL-R (rabbit against human) and GM 130 (mouse against human) were purchased from Abnova (Paderborn, Germany) and BD Biosciences (Heidelberg, Germany), respectively, and used in a dilution of 1:100 in 1 % BSA (diluted with PBS). Secondary antibodies Alexa Fluor 488 (anti rabbit) and Alexa Fluor 568 (anti mouse) were purchased from Life Technologies (Darmstadt, Germany) and used in a dilution of 1:700 in 1 % BSA (diluted with PBS).

### **Results**

#### Hepatic phenotype

All patients had fever-dependent episodes of ALF (Fig. 1a). The first episode of ALF occurred mostly in infancy (mean 12.7 months, range 4-24 months); patient 8 had her first liver crisis at the age of 6.7 years (Table 1). Characteristically, patients presented with recurrent vomiting and increasing lethargy 1 or 2 days after the onset of fever. ALF episodes usually started with massively elevated ALAT and ASAT, succeeded by severe coagulopathy and mild to moderate jaundice. Alkaline phosphatase and gamma-GT were normal or only slightly elevated (see Table 2). Hypoglycemia, hyperammonemia, and hepatic encephalopathy were transiently observed in some patients. Some patients had transient hepatomegaly during crises that normalized in the interval. If the liver crisis was survived, liver function always recovered completely within days or weeks and remained normal in the interval. All patients had recurrent liver crises and all but three patients had at least two episodes that fulfill criteria of an ALF, therefore presenting RALF. The frequency and severity of ALF was highest during infancy and early childhood, when virtually all febrile infections, including vaccinations, led to ALF (Fig. 1b). In five patients, the first



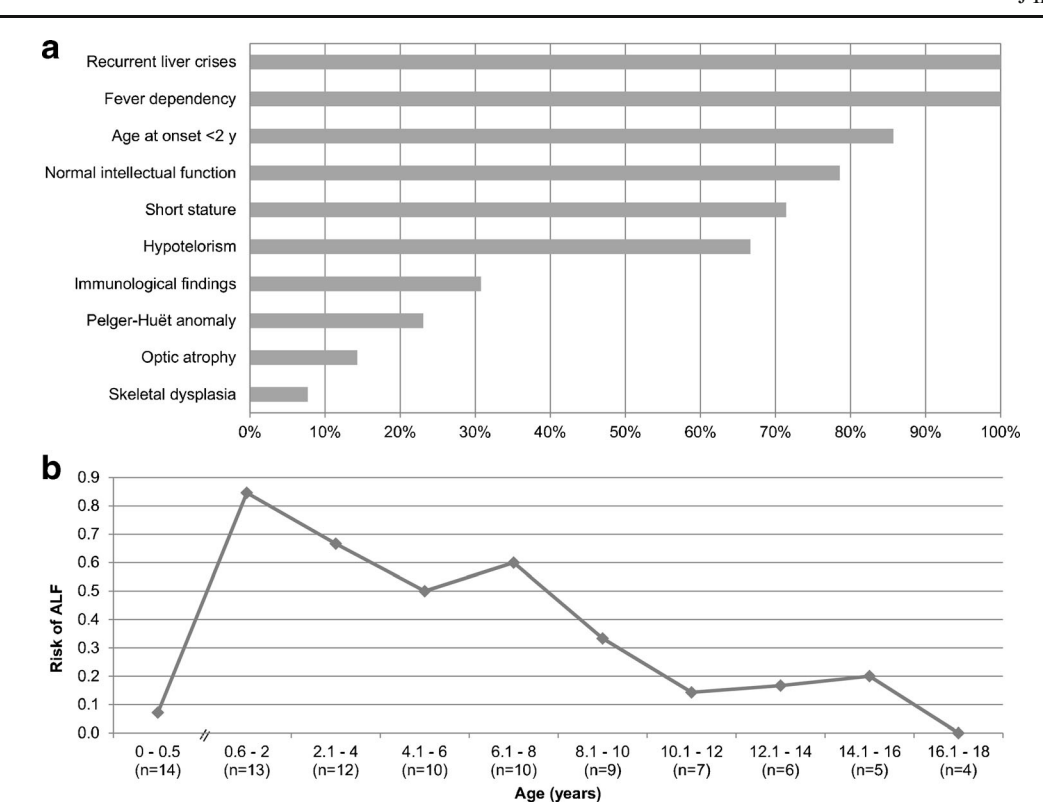


**Fig. 1** Clinical signs and symptoms and frequency of ALF according to age **a** Clinical signs and symptoms. All patients presented a hepatic phenotype characterized by recurrent liver crises that mostly lead to acute liver failure, therefore presenting RALF. Hypotelorism and short stature are the most frequent extrahepatic findings. Data of patients 1–14 are included. **b** Distribution of ALF according to age. The risk of having ALF is shown (n of patients with ≥1 ALF in a given age group/total n of patients in that age group). The total number of ALFs represented in this figure is 65. The risk of having ALF is highest between 0.6 and 2 years

(0.85) and decreases with age but is not restricted to childhood. This reflects exposure to infections in infancy and early childhood. The risk is still relatively high between 6.1 and 8 years (0.60) but then decreases. The latest crisis occurred in patient 2 at age 21 years (not shown in the figure). With increasing age, febrile infections mostly lead to no or a milder hepatic phenotype without ALF (not documented in the figure). For patient 4, exact data are missing from age 0.6 to 18 years. Data of patients 1–14 are included

ALF episode was also the most severe. With increasing age, not all febrile infections led to crises, in particular with refinement of therapy. After the age of 10 years fever more often caused no or only a mild hepatic phenotype with (slightly) elevated ALAT but without coagulopathy and jaundice.

In two families (family FVIII and FIX, Table 1), the oldest siblings had died in early childhood (aged 14 and 11 months) due to febrile-associated ALF of at that time unknown cause. No material was available to genetically confirm mutations in *NBAS*. Patient 10 received a liver transplant at the age of 3 years after three episodes of ALF and death due to ALF of an older sister.

In the interval and at the time of study visit, all patients had normal ALAT and ASAT and normal liver function parameters. Hepatic morphology studied by ultrasound was unremarkable in all patients, except in patient 12 in whom two small hepatic lesions were seen with some irregular aspect of liver borders. Transient elastography was studied in patients 1–5 and was normal except for the oldest patient, who had

increased liver stiffness (8.7 kPa, normal 3.9–5.3 kPa (Kim et al 2010)) at the age of 37 years (patient 4).

Detailed metabolic work-up during crises and in the interval including blood gas analysis and blood lactate, ketones in urine, acylcarnitine profiles in dried blood spots, amino acids in plasma and organic acids in urine, always showed normal or non-specific results. There was no evidence for primary or secondary dysfunction of intermediary, mitochondrial, peroxisomal or lysosomal metabolism, cholesterol and glycoprotein biosynthesis or any of the other hitherto known specific causes of ALF.

### Therapeutic management of ALF

Therapy was optimized and tailored by growing clinical experience in recurrent crises, resulting in a specific emergency protocol. Early and effective control of fever often allowed prevention of liver crises, whereas parenteral application of high glucose (10–12 g/kg body weight and day in infants) ameliorated the course, especially if started early in the course.



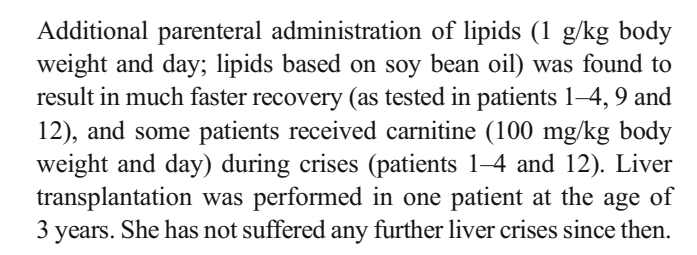
Table 1 Clinical data of patients with NBAS deficiency

General data								Henatic phenotype	henotype				
ID	Sex <sup>a</sup>	Nationality	Age at last visit <sup>a</sup>	Genotype <sup>a</sup> (mutati	(mutations	ons in NBAS)		Number of ALF <sup>a</sup>	Number of liver crises without ALF	Age at onset <sup>a</sup>	Age at last ALF <sup>a</sup>	Age at most severe crisis	ALF fever dependent
Pat 1 (F1) Pat 2 (F11) Pat 3 (F111) Pat 4 (F1V) Pat 5 (FV) Pat 6 (FV) Pat 6 (FV) Pat 8 (FV) Pat 9 (FV) Pat 10 (F1X) Pat 11 (FX) Pat 11 (FX) Pat 12 (FX) Pat 13 (FX) Pat 14 (FX) Pat 15 (FX) Pat 15 (FX) Pat 15 (FX) Pat 16 (FX)		DE D	18 y 18 y 18 y 18 y 19 y 10 y 11 y 11 y 18 y 18 y 16 y 16 y 17 y 18 y 18 y 18 y 18 y 18 y 18 y 18 y 18	c.[558_5604 c.[2708_T>(603_6054 c.[3010C>T>(613_5154 c.[1042C>T] c.[118-7C>T] c.[118-7C>T] c.[118-7C>T] c.[118-7C>T] c.[18-7C>T] c.[2827G>T] c.[2827G>T] c.[173-2C>T] c.[173-2C>T] c.[173-2C>T]	lel];[686dup] G];[2768 T> tel];[3164 T G];[2876- [1];[4 T>0 F];[3164 T>0 F];[2203 3C F];[2203 3C F];[2	c.[558_560del];[686dup], p.[Ile187del];[Ser230Glr.c.[2708_T-9];[2108_T-9], p.[Leu203Arg];[Leu9.c.[603_605del];[3164_T-C], p.[Leu202del];[Leu16.c.[2708_T-9];[2827G-T], p.[Leu903Arg];[Glu94.c.[3010C-T];]3164_T-C], p.[Heg104**], p.[He512Thrfs*4]; c.[1042C-T];[2203_3C-G], p.[Pro348Ser];[7]; c.[1042C-T];[2203_3C-G], p.[Pro348Ser];[7]; c.[1187G-A];[2330C-A], p.[Tay36*];[Pro77THi.c.[118.c.A-G];[2524G-T], p.[CiyMal84Phe]; c.[686dup];[3164_T-C], p.[Ser230Glnfs*4];[Leu16.c.[2827G-T];[exons_39-40_del], p.[Glu943*]; [Vac.[173-2A-G];[353A-G], p.[-1], p.[Ala95Va]];[Ile1121Met] c.[244C-T];[850A-T], p.[Ala95Va]];[Ilys284Ter] c.[409C-T];[1186_T-A], p.[Ala95Va]];[Typ396, c.[124C-T];[Roland T], p.[Ala95Va]];[Typ396, c.[409C-T];[Typ396, p.[Ala95Va]];[Typ396, c.[409C-T]];[Typ396, c.[409C-T];[Typ396, p.[Ala95Va]];[Typ396, c.[409C-T]];[Typ396, c.[409C-T];[Typ396, c.[409C-T]];[Typ396, c.[409C-T]];[Typ306, c.[409C-T]];[Typ3	c.[558_560del];[686dup], p.[IIe187del];[Ser230Glnfs*4] c.[2708_T>G];[2708_T>G], p.[Leu903Arg];[Leu903Arg] c.[603_605del];[3164_T>C], p.[Leu202del];[Leu1055Pro] c.[2708_T>G];[2827G>T], p.[Leu903Arg];[Glu943*] c.[3010C-T;[3164_T>C], p.[Leu903Arg];[Glu943*] c.[3010C-T;[3164_T>C], p.[Leu903Arg];[Glu943*] c.[1042C>T;[3203_3C>G], p.[Pro348Ser];?] c.[1042C>T;[2203_3C>G], p.[Pro348Ser];?] c.[1042C>T;[2203_3C>G], p.[Pro348Ser];?] c.[1187G>A];[2330C>A], p.[Th396*3;[Pro77THis] c.[1187G>A];[2330C>A], p.[Th396*4];[Leu1055Pro] c.[1684Dp];[3164_T>C], p.[Ser220Glnfs*4];[Leu1055Pro] c.[2827G>T];[exons_39-40_del], p.[Glu943*]; [Val1528Glyfs*2] c.[173-2A-G];[353AA-G], p.[-];[Ile1121Met] c.[284C>T];[850A>T], p.[Arg137Tp];[Th396Arg] c.[409C>T];[1186_T>A], p.[Arg137Tp];[Th396Arg]	2 7 7 7 7 7 7 7 7 7 7 7 7 7 7 7 7 7 7 7	112 8 8 8 8 8 8 1 1 2 1 2 1 3 1 3 1 3 1 3 1 1 1 1 1 1 1 1 1 1 1 1	21 m 10 m 8 m 8 m 18 m 11 m 6.7 y 6.7 y 6.7 y 7 m 7 m 7 m	14.8 y 21.1 y 11.6 y n.a. 9.8 y 3.9 y 6.6 y see first crisis 3.3 y 5.8 y 1.7 ys 6 y 5.8 y 1.7 ys 1.4 y n.a.	1.8 y (first crisis) 3.8 y 10 m (first crisis) n.9 1.9 y 2.8 y 11 m (first crisis) 3.1 y 2.2 y 1.4 y 1 y 6 y 2.0 y (first crisis) n.a. n.a.	yes yes yes yes yes yes yes yes yes yes
General data	Extral	Extrahepatic phenotype	otype										
n n	Short (SDS)	stature	Skeletal Hyg dysplasia	Hypotelorism C	Optic F atrophy a	Pelger Huët anomaly	Immunological findings	Neurologic	Neurological examination Intellectual performance	Intellectual pe		Other pathological findings, comorbidities <sup>a</sup>	ndings,
Pat 1 (FI)	ves (-2.67)	2.67) no	ves		ves (mild) n	no	по	normal		normal (IO 112)		ou	
Pat 2 (FII)	yes (-2.08)	2.08) no	yes			no	no	normal		LD (IQ 77)		acute renal failure, epilepsy	epsy
Pat 3 (FIII)	yes (-4.24)	4.24) no	yes		n on	no	Celiac disease <sup>a</sup>	normal		normal (IQ 111)		ou	
Pat 4 (FIV)	yes (-2.25)	2.25) no	yes		n on	no	no	mild coording	mild coordination deficit	ID (IQ 50)	-	no	
Pat 5 (FV)	no (0.22)	22) no	yes		n on	no	no	normal		normal (IQ 97)		mild cardiomyopathy	
Pat 6 (FVI)	yes (-2.91)	2.91) no	n.a.		no n	n.a.	no	mild motor delay	delay	normal (IQ n.a.)		no	
Pat 7 (FVII)	no (0.6)	ou (9	yes		n on	n.a.	no	normal		normal (IQ 92)	-	no	
Pat 8 (FVII)	yes (-2.71)	2.71) no	no	и	no y	yes	erythema nodosum, Crohn's disease	normal		upper normal (IQ 124)		no	
Pat 9 (FVIII)	no (-0.63)	ou (63)	no	и	n on	n.a.	no	normal		normal (IQ n.a.)		no	
Pat 10 (FIX)	yes (-2.62)	2.62) no	n.a.		n on	n.a.	no	normal		normal (IQ n.a.)		episodes of mild hypoglycemia during acute illness	glycemia
Pat 11 (FX)	yes (-2.35)	2.35) no	n.a.		u ou	n.a.	no	normal		normal (IQ n.a.)		ou	
Pat 12 (FXI)	yes (-2.48)	2.48) yes	no	λ	yes y	yes	lymphopenia during crisis,	Left hemi-paresis, mild	aresis, mild	mild psycho-motor delay		neuroblastoma, epilepsy	ý
Pat 13 (FXII)	yes (-2.07)	2.07) no	n.a.		no y	yes	hypogammaglobulinemia	nypotoma	4	normal (IQ n.a.)		no	
Pat 14 (FXIII)	no (-1.15)	.15) n.a.	ou	u	u ou	n.a.	n.a.	normal		normal (IQ n.a.)		no	
Pat 15 (FXIV) <sup>b</sup>	yes (-3)	3) yes	n.a.		yes	yes	bulinemia, ral killer cells, to	normal		normal (IQ n.a.)		cervical instability, redundant skin, reduced subcutaneous fat	undant skin, us fat
							vaccinations						



General data	General data Extrahepatic phenotype	phenotype							
OI OI	Short stature (SDS)	Skeletal dysplasia	Short stature Skeletal Hypotelorism SDS) dysplasia	Optic atrophy	Pelger Huët anomaly	Immunological findings	Pelger Huët Immunological findings Neurological examination Intellectual performance Other pathological findings, anomaly	Intellectual performance	45
Pat 16 (FXV) <sup>t</sup>	at 16 (FXV) <sup>b</sup> yes (-3.5) yes	yes	n.a.	ou	yes	reduced natural killer cells	motor development initially n.a. retarded, mild speech	n.a.	

Pat 1 L-Patient 1 family I, F female, M male, two letter code for nationality (ISO 3166-1), y years, m months, IQ intelligence quotient, LD learning disability, ID intellectual disability, DD developmental delay, n.a. not available, SDS standard deviation score



## Extrahepatic phenotype

The majority of patients with mutations in *NBAS* reported in this article have short stature (10/14), with a mean supine length of -2.64 SDS (Table 1 and Table S1). In some individuals, reduced pubertal growth spurt was noted. One patient presents with a skeletal phenotype including osteopenia (patient 12), while there are only minor or no skeletal symptoms in the other patients (Fig. 2). Minor facial dysmorphism including hypotelorism is observed in most patients, regardless of other skeletal abnormalities. Four patients present immunological findings or autoimmune diseases. Abnormalities of other organ systems include optic atrophy and Pelger-Huët anomaly, acute renal failure (during ALF), mild hypertrophic cardiomyopathy, and epilepsy.

Remarkably, one patient had a renal neuroblastoma that was diagnosed at the age of 1 month (patient 12). Nephrectomy was performed at the age of 7 months (preceded by chemotherapy) and histology classified the neuroblastoma as differentiated neuroblastoma, Schwannian stroma-poor, according to the International Neuroblastoma Pathology Classification.

Patient 12 suffered a haemorrhagic cerebral insult during an ALF episode with severe coagulopathy at the age of 1 year resulting in left hemiparesis and epilepsy. His development is mildly retarded, he has muscular hypotonia and poor speech, but he progresses nevertheless and sits alone, handles toys and interacts nicely with his mother. In the other patients, neurological examination was unremarkable except a minor coordination deficit in patient 4 and mild motor delay in patient 6. IQ was normal in most patients and below the normal range in three patients. MRI (patients 1–6, 10, and 12) revealed unspecific patterns of mild brain atrophy in six patients (1–4, 6, and 12) (mild supratentorial white matter deficit and/or mild atrophy of the superior vermis) and was normal in the others, <sup>1</sup>H-MRS studies in patients 1–4 revealed normal results.

# Morphological characterization of hepatocytes and fibroblasts

The most prominent finding on liver biopsies, especially when biopsies were taken shortly after crises, was microvesicular steatosis, and regeneration phenomena with pseudo-rosetting of hepatocytes (Fig. 3a, b). In ultrastructural analysis of liver biopsies of patients 1, 2, 5, and 7, besides microvesicular steatosis hepatocytes showed increased and enlarged ER, but normally appearing, apically oriented Golgi (Fig. 3c). Immunohistochemical analysis



<sup>&</sup>lt;sup>a</sup> Data regarding patients 1–11 published before (Haack et al 2015)

<sup>&</sup>lt;sup>b</sup> Patients published by (Garcia Segarra et al 2015)

 Table 2
 Laboratory data of patients with NBAS deficiency (maximum values during most severe ALF episode)

ID III	Age at most severe crisis	ALAT (U/L)	ASAT (U/L)	Total bilirubin (µmol/L)	Direct bilirubin Gamma-GT AP (µmol/L) (U/L)	Gamma-GT (U/L)	AP (U/L)	AP NH3 Blood gluc (U/L) (µmol/L) (mmol/L) <sup>a</sup>	Blood glucose (mmol/L) <sup>a</sup>	Lactic acid (mmol/L)	Blood glucose Lactic acid INR/PT/Quick's value <sup>b</sup> (mmol/L) <sup>a</sup> (mmol/L)	HE (Grade)
Pat 1 (FI)	1.8 y	0609	9892	46.9	28.7	53	454	122	n.a.	3.1	Quick's value 19 %	no
Pat 2 (FII)	3.8 y	0599	6012	132.6	74.8	168	n.a.	190	1.9	2.7	Quick's value 7 %	yes (IV)
Pat 3 (FIII)	0.8 y	4160	3510	85.0	n.a.	normal	n.a.	98	normal	normal	Quick's value <10 %	yes (IV)
Pat 5 (FV)	1.9 y	6400	9200	124.1	71.4	40	707	113	1.1	3	Quick's value <10 %	yes (IV)
Pat 6 (FVI)	2.8 y	11,464	24,721	46.8	n.a.	87	1241	173	3.2	9.6	INR 10	yes (III)
Pat 7 (FVII)	0.9 y	12,230	8920	73.1	n.a.	84	n.a.	99	0.4	n.a.	Quick's value 6 %	yes (III)
Pat 8 (FVII)	6.7 y	11,800	10,880	85.0	n.a.	142	n.a.	209	3.2	3.1	Quick's value 11 %	yes (III)
Pat 9 (FVIII)	3.1 y	4001	7388	2.69	n.a.	50	n.a.	82	5.2	4.2	INR 5.6	yes (I–II)
Pat 10 (FIX)	2.2 y	17,700	22,040	207.4	49.3	25	372	136	3.8	2.3	INR 13.4	yes (III)
Pat 11 (FX)	1.4 y	n.a.	17,150	52.7	39.1	n.a.	1250	n.a.	n.a.	n.a.	PT 98.1 s	n.a.
Pat 12 (FXI)	1 y	8966	5114	227.8	35.7	144	501	100	0.5	5.4	Quick's value <10 %	yes (IV)
Pat 13 (FXII)	6 y	11,198	16,650	76.5	73.4	99	300	96	n.a.	0.2	INR 2.4	no
Pat 14 (FXIII)	2 y	6373	11,110	233	170	56	290	198	3	10.2	Quick's value 7 %	yes (I–II)
Reference values	es	<50	<50	<20	<3.4	<50	<390	<54	3.3–6.9	0.5-2.2	INR <1.2, Quick >70 %, PT 11-14 s	

HE hepatic encephalopathy, AP alkaline phosphatase, NH3 blood ammonia, PT prothrombin time

<sup>a</sup> Minimum value

<sup>b</sup> Most ALF episodes occurred up to 20 years ago when Quick's value or prothrombine time (PT) were generally used (instead of INR). Patient 4 (FIV) not included, as detailed laboratory values are not available





**Fig. 2** Morphological characteristics of NBAS-deficient patients **a** Patients 1–5 represent the group of patients with a hepatic phenotype without skeletal dysplasia. However they have very mild morphological characteristics, such as long facies, hypotelorism, and flat cheekbones. **b** Patient 12, at the age of 14 months. He suffered a hemorrhagic cerebral insult during an ALF episode at the age of 1 year and has a left sided hemiparesis since then. He is short of stature (-2.48 SDS), has enophtalmia, brachydactyly, and clinodactyly of the fingers two and

four of both hands. The 4th fingers are longer than the 3rd. The X ray of the right forearm and hand at the age of 8 months shows osteopenia with thin corticalis, an additional ossification center at the base of the 3rd finger and retarded ossification of the carpus (all present bilaterally). X ray of the skull (age 8 months) shows a steep clivus and a relatively prominent neurocranium related to the viscerocranium. The X ray of the right foot (age 14 months) demonstrates missing ossification of the middle and end phalanx of the 5th toe

of NBAS in liver biopsies revealed a diffusely cytoplasmic to granular pericanalicular staining as demonstrated in patients 1, 6, and 7, but was much less intense or even absent in comparison to liver biopsies of control patients with microvesicular steatosis of other etiology (Fig. 3d, e). Positive cytokeratin 7 staining in patient 10 highlights ductular proliferations and ductular metaplasia of periportal hepatocytes as signs of extra acinar cholestasis, indicating chronic liver damage concomitant to portal and periportal fibrosis (Fig. 3f, biopsy taken during ALF), whereas there are no signs of fibrosis in the other patients. Mitochondria showed dense matrix and abnormal internal architecture with dilated, elongated cristae and rare targetoid cristae in the same

patient (Fig. 3g), whereas only mild mitochondrial abnormalities were detected in the other patients examined.

In fibroblasts of patients and controls, NBAS staining was observed at cytoplasmic vesicles, in partial colocalization with ER markers, but not colocalizing with the Golgi marker GM130 or with lipid droplets stained by BODIPY or perilipin 2 (data not shown).

### Functional characterization of fibroblasts

*NBAS* mutations result in decreased intracellular protein levels of NBAS, indicating substantial impairment of protein translation



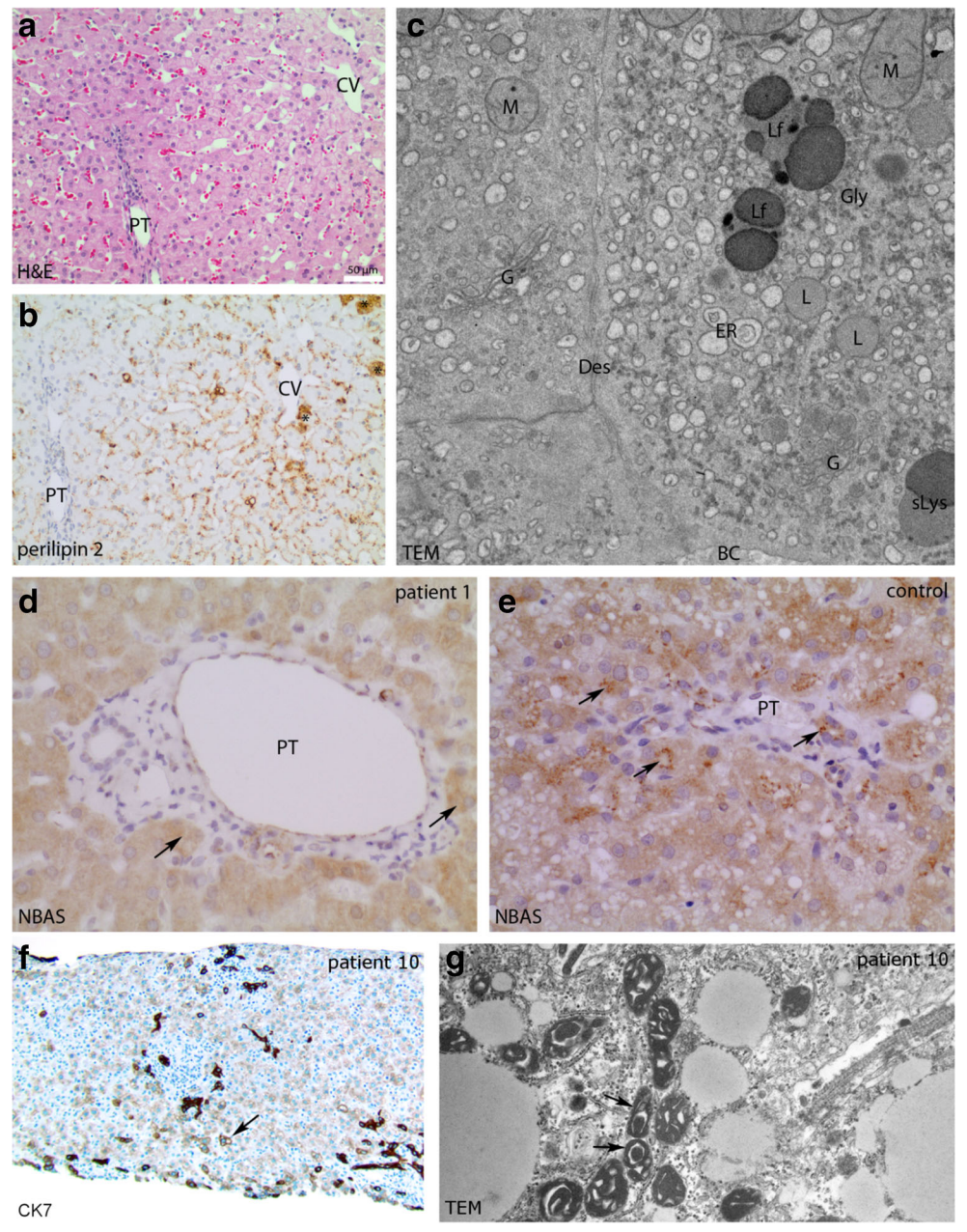


Fig. 3 Deficiency of NBAS results in microvesicular steatosis, dilation of ER and aberrant mitochondria in liver **a**–**d** liver biopsy of patient 1, taken 7 weeks after last crisis. **a** Conventional H&E morphology showing microvesicular steatosis and pseudorosetting of hepatocytes. **b** Microvesicular steatosis of the liver as demonstrated by immunohistochemical analysis with antibodies against the lipid droplet-associated protein perilipin 2. *Asterisks*: extensive microvesicular steatosis in singular perivenous hepatocytes. **c** Ultrastructural analysis of glutaraldehyde-fixed material showing hepatocytes with extensive dilation of the ER, lipid droplet-accumulation and peripherally oriented Golgi apparatus and mildly abnormal mitochondria (20,000×). **d**, **e** Immunohistochemical analysis demonstrates faint cytoplasmic NBAS-staining in patient 1 (**d**), whereas in control patients with microvesicular

steatosis (e), prominent vesicular NBAS-staining is observed (*arrows*) (400×) f, g liver biopsy of patient 10, taken during first episode of acute liver failure. f Cytokeratin 7 stain showing dark brown profiles of bile ducts and ductular reaction. Some hepatocytes demonstrate lighter staining and are a transitional phenotype between hepatocyte and cholangiole (neocholangiolization) (*arrow*) (cytokeratin 7, 100×). g Mitochondria demonstrate dense matrix and abnormal internal architecture with dilated, elongated cristae and rare targetoid cristae (*arrows*) (24,700×). *Abbreviations*: H&E Hematoxylin and eosin stain; TEM transmission electron microscopy; PT portal tract; CV central vein; M mitochondrium; Des desmosome; BC bile canaliculum; L lipid droplet; ER endoplasmic reticulum; Gly glycogen rosettes; Lf lipofuscin; G Golgi apparatus; sLys secondary lysosomes; CK7 cytokeratin 7

and/ or protein stability in all patients investigated. Decreased NBAS protein was paralleled by a reduction of p31. As fever is a necessary starting point for ALF in patients

with *NBAS* mutations, we challenged patients' fibroblasts by a temperature shift from 37 to 40 °C. After the temperature shift, a further decrease of the levels of NBAS as well as p31



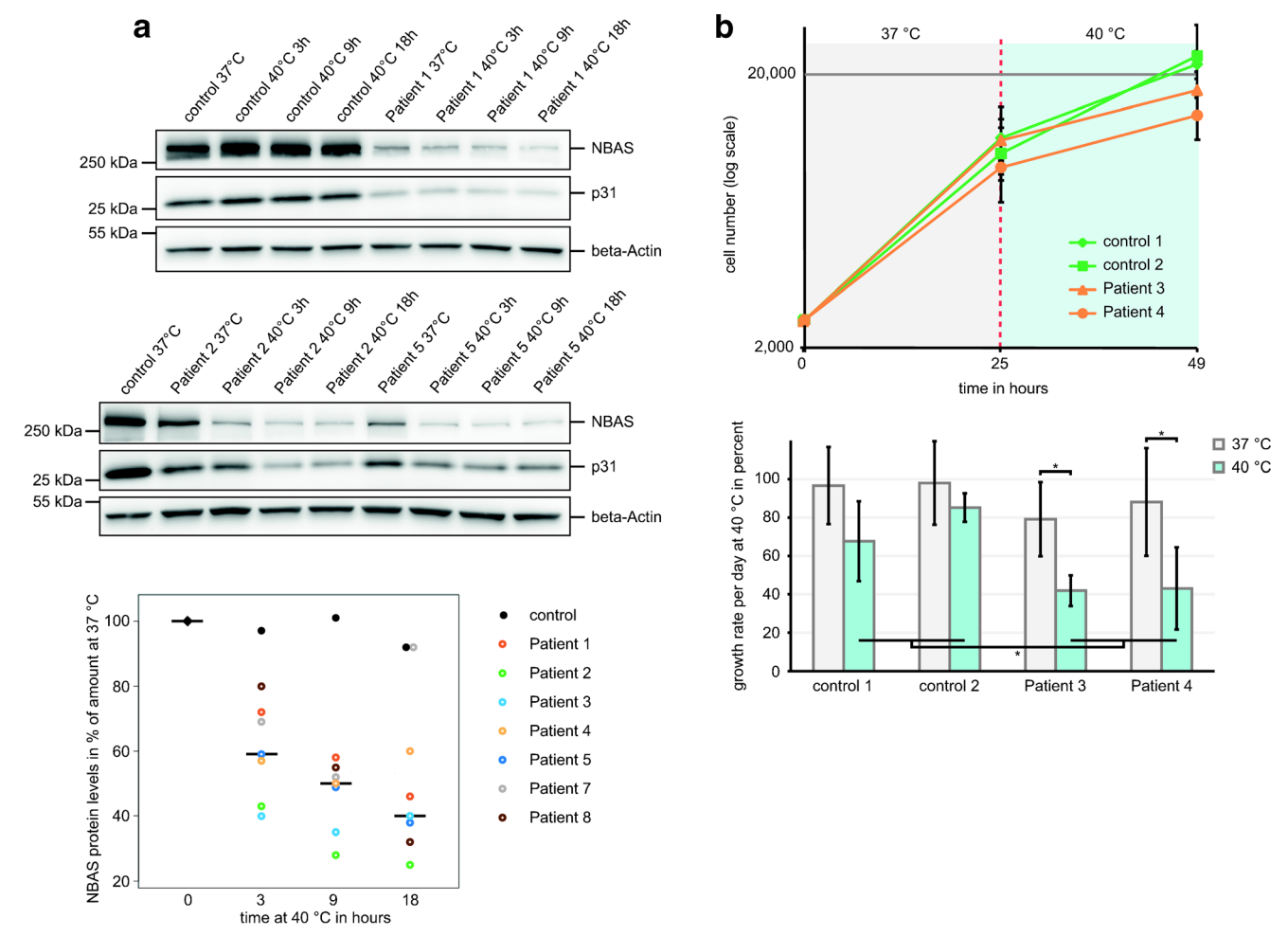


**Fig. 4** Thermal susceptibility of the syntaxin 18 complex. **a** Decrease in NBAS and p31 protein levels at 40 °C. Patient and control fibroblast cell lines were cultivated at 37 °C and then heated to 40 °C. Cells were collected at different time points and investigated for NBAS and p31 protein levels. In control cell lines, NBAS and p31 levels remained unchanged at all conditions. In all patient cell lines, NBAS protein levels significantly decreased after the temperature shift to 40 °C (3 h: p=0.0026; 9 h: p<0.0009; 18 h: p=0.0038; two-tailed paired t-test; representative images shown for three out of eight patient cell lines). Quantification of protein levels for each cell line are given in the diagram on the right expressed as the relative amount of NBAS after several hours of incubation at 40 °C in comparison to 37 °C. Black dots indicate levels of control cell lines. Colorful points indicate levels for seven patient cell lines. The black line indicates the median level of

NBAS in patient cell lines. **b** Impaired growth of patients' fibroblasts at 40 °C. Growth of fibroblast cell lines of two patients (3 and 4) and two controls at 37 and 40 °C, respectively; 2500 cells of patient and control fibroblast cell lines were cultivated at 37 °C. After 25 h, some plates were placed in 40 °C and left for an additional 24 h. Cell growth was assessed by quantification of DNA in three independent experiments with three replicates each time. Growth rates are expressed as percent increase per day. Stars (\*) indicate a significant difference ( $p \le 0.05$ ). While there was no significant difference in growth rates between patient and control cell lines at 37 °C (p = 0.224), patient cell lines grew significantly slower than control cell lines at 40 °C (p = 0.037). In addition, only patient cell lines displayed a significant impairment of growth rate at 40 °C compared to 37 °C (for patient 3: p = 0.045; for patient 4: p = 0.018; both two-tailed paired t-test)

by half occurred in patients' fibroblasts (Fig. 4a). The observation that NBAS levels remain constant in control cell lines after the same temperature shift while decreasing in patient cell lines indicates specific mutation-dependent thermal instability of the NBAS protein in patients. Growth rates of patient and control cell lines were indistinguishable at 37 °C, but the temperature shift from 37 to 40 °C resulted in a significant decrease of growth rates in patient cell lines only (Fig. 4b). Hence, the mutations in *NBAS* resulted in temperature sensitive loss of SNARE complex subunits accompanied by a reduction of vital fitness in fibroblasts.

To further asses a potential impact of NBAS depletion on the cellular distribution of proteins, immunofluorescence analyses dependent on digitonin permeabilization were performed. Digitonin is known to permeabilize the plasma membrane but not ER and Golgi membranes (Aoki et al 2009). Double staining of control and patient-derived fibroblasts with antibodies against ERGIC-53 and GPP130 revealed a markedly reduced intensity of fluorescence in patients cells after treatment with digitonin, while control cells remain widely unaffected (Fig. 5). This indicates that ERGIC-53- and GPP130-containing membranes are not tightly bound in NBAS-depleted cells and thus



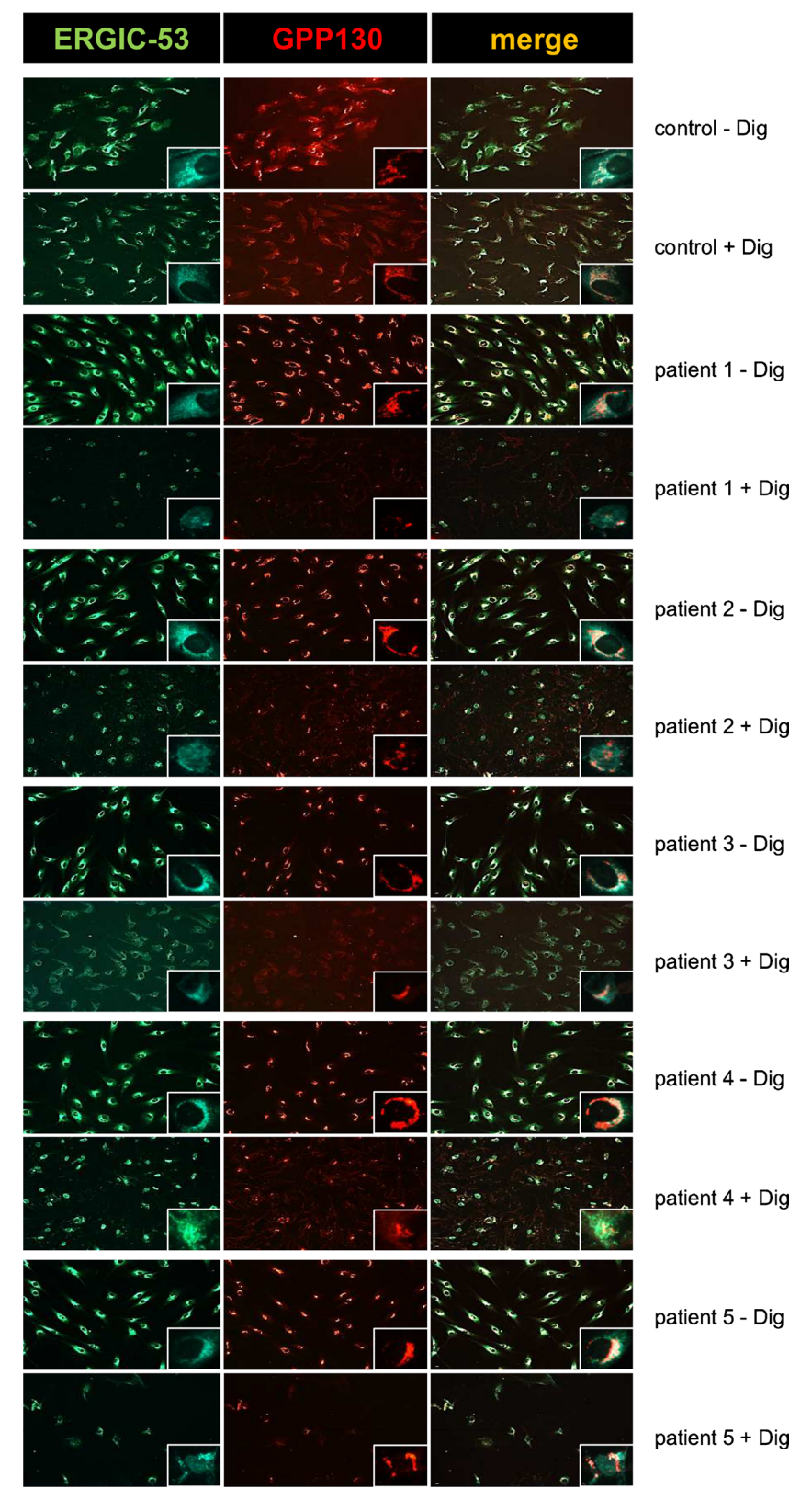


Fig. 5 Impaired tethering of vesicles in patients' fibroblasts. Distribution of ERGIC-53 in digitonin-permeabilized and non-permeabilized cells. Localization of ERGIC-53 (green, left column) and GPP130 (red, middle column) were examined by immunofluorescence double

labeling of fibroblasts. The *right* column shows the combined results of all three images (merge), respectively. Magnification is  $20^{\times}$ . The *box* shows a representative cell with  $40^{\times}$  magnification. Scale bar: 10  $\mu m$ . - Dig, without digitonin; +Dig, with digitonin



are released from digitonin permeablized cells, suggesting a defective tethering of corresponding vesicles. In a second approach we investigated the localization of KDEL-R in combination with GM130 and found the same effect in the patients' fibroblasts treated with digitonin, albeit the outcome was not so pronounced as observed for ERGIC-53 (data not shown).

# **Discussion**

RALF caused by mutations in *NBAS* is a new and presumably frequent inherited cause of pediatric ALF. Fever was found to be necessary, but not sufficient to cause ALF. In the interval, liver function recovers completely. Crises are precipitated by vomiting and lethargy and start rather uniformly with massively elevated ASAT and ALAT, followed by a functional deficit leading to coagulopathy. Hyperammonemia and hypoglycemia occurred secondarily during ALF. Early and consequent administration of antipyretics together with anabolic energy management through application of high glucose and lipids proved to be highly beneficial gathered through up to 20 years of personal follow-up and experience in different centers. Episodes of ALF can be diminished to mild hepatopathy or even completely prevented with this therapeutic approach if implemented before ASAT and ALAT are massively elevated.

The phenotypic variability of the patients highlight that mutations in NBAS lead to a clinical spectrum ranging from isolated RALF to a multisystemic phenotype including short stature, skeletal dysplasia, optic atrophy, and immunological abnormalities, but also minor syndromic features such as hypotelorism. SOPH syndrome represents part of that spectrum, although interestingly no liver phenotype has been described in the affected patients. High comorbidity in NBAS deficiency points to an association of further pathologies, such as cardiomyopathy, renal failure, or epilepsy. Motor and cognitive development was normal in most patients, independent of the extrahepatic comorbidities and despite recurrent severe liver failure episodes. The neurological features and mild MRI abnormalities observed in some patients could be explained as sequelae of ALF, however a primary neurological phenotype cannot be ruled out completely. The phenotypic spectrum of NBAS deficiency will be further clarified by the identification of new patients and their detailed clinical characterization. A recent report of two patients with NBAS deficiency underlines the wide spectrum of the disease (Garcia Segarra et al 2015) (Table 1).

One of the patients developed neuroblastoma and it is tempting to speculate that mutations in *NBAS*, initially described as a gene coamplified with N-myc in neuroblastoma tumor cells, predispose for neuroblastoma. However, this remains to be elucidated.

The exact mechanism of liver failure in NBAS deficiency is unclear and the physiologic function of NBAS remains to be further clarified. As far as is understood, NBAS plays a role in retrograde transport between ER and Golgi in yeast and humans (Aoki et al 2009). Notably, we have recently shown a concomitant reduction of p31 (Haack et al 2015), providing further evidence that both proteins are subunits of the same SNARE complex. We now demonstrate thermal susceptibility of the syntaxin 18 complex in cultivated patients' skin fibroblasts, which suggests that raised temperature itself may be the starting point of a derailment. In Mendelian disease, temperature sensitive mutations are not rare.  $\Delta$ F508-CFTR, the most common disease-causing mutation resulting in cystic fibrosis, also results in a temperature sensitive folding defect (Ward et al 1995).

Tethering of vesicles associated with ER/Golgi transport is affected in patients' fibroblasts, supporting a role of NBAS in retrograde transport. In line with this finding, ER morphology in hepatocytes as determined in transmission electron microscopy was found to be altered. Dilation of smooth ER may be a non-specific sign of hepatic injury (Lossie et al 2014), but a similar vacuolated ER structure was found in p31-depleted mouse embryonic fibroblast cells (Uemura et al 2009) and gross dilation of the ER was shown in fibroblasts from individuals affected with cranio-lenticulo-sutural dysplasia, a defect of anterograde transport due to mutations in SEC23A (a component of the COPII-coated vesicles that transport secretory proteins from the ER to the Golgi complex) (Boyadjiev et al 2006). Altered ER has been shown to induce ER stress and apoptosis in p31-depleted cells (Uemura et al 2009), and in NBAS-mutant fibroblasts a significant increase in the expression of genes involved in ER stress response was found (Haack et al 2015). We hypothesise that fever-dependent ALF is the common final path of ER stress-induced liver cell apoptosis, which is set off by temperature-dependent NBAS and p31 depletion.

Therapeutic experience shows that ALF can be prevented through early and effective antipyretic therapy, which is congruent with our in vitro findings. The observed positive effect of intravenous application of glucose and lipids cannot be explained easily. Intestinal fat absorption has been shown to be related to the COPII-machinery (Jones, Jones et al 2003) and it may be speculated whether there is an (intermittent) effect on enteral fat absorption due to disturbed vesicular transport mechanisms in NBAS deficiency, which could be bypassed by parenteral application of lipids. However, this would not explain the observed effect of lipids on decelerating liver failure. Liver transplantation may be considered as therapeutic option to prevent further ALF episodes in NBAS deficiency; however conservative treatment together with the natural history of disease will leave transplantation as treatment of last resort. SOPH syndrome presents the other facet of the phenotypic spectrum of NBAS deficiency. No hepatic phenotype was hitherto reported in these patients who all share the same homozygous missense mutation (p.Arg1914His) in the C-terminal domain of unknown function (Maksimova et al 2010). The impact of this mutation on protein function is unknown. Notably, most patients with



hepatic phenotype have mutations in the sec39 domain of NBAS (amino acids 725–1376) or have mutations located before this domain (Table 1, (Haack et al 2015)) which may lead to a truncated protein.

In addition to its role in retrograde vesicular transport, NBAS is thought to act as a mediator of the nonsensemediated mRNA decay (NMD) and was shown to modulate genes involved in cholesterol biosynthesis and bone development (Longman et al 2013). Longman et al already speculated that a dysfunction of NBAS in NMD processes could explain skeletal dysplasia and Pelger-Huët anomaly as described in SOPH syndrome. Depending on the functional consequences of NBAS mutations, the NMD function of NBAS may become affected to different degrees, resulting in a distinct grade of regulation of, e.g., bone metabolism and therefore skeletal involvement. The multisystemic phenotype of NBAS deficiency is reminiscent of defects of cholesterol biosynthesis whose genes are affected by NBAS-mediated NMD as well. We have found no biochemical abnormalities of cholesterol biosynthesis in our patients, however an intermittent deregulation of cholesterol biosynthesis cannot be ruled out.

In up to 50 % of children with ALF the cause remains undetermined. A significant proportion of these children may have an underlying genetic disorder or predisposition. As new patients have been quickly identified after the identification of the causative gene, NBAS deficiency seems to be a frequent cause of RALF, and it may also be a frequent cause for recurrent, milder liver crises not fulfilling criteria of an ALF or isolated ALF in children. Extrahepatic symptoms or comorbidities such as short statue, skeletal dysplasia, hypotelorism or optic atrophy may help to identify NBAS deficiency as the underlying cause of an unexplained ALF, but patients may have no other symptoms apart from hepatic involvement. As there is no specific laboratory marker, diagnosis of NBAS deficiency relies on genetic testing. The analysis of NBAS protein levels via immunohistochemistry of liver biopsy or western blot analysis of fibroblasts may help in the diagnostic process. Specific treatment with glucose and lipid infusion ameliorates the course of ALF and early antipyretic therapy is rationally based on the demonstrated thermal susceptibility of the syntaxin 18 complex. Although complete recovery from liver crises is usually found, ALF can be lethal in individual patients. Identification of NBAS deficiency in patients with ALF allows optimized therapy and can even facilitate prevention of further ALF episodes.

**Acknowledgments** The authors thank Lena Pawella, Elisabeth Specht-Delius, Eva Eiteneuer, Marion Hahne, Zlata Antoni, Lena Protzmann, and Sabine Schäfer for excellent technical assistance. Human control tissues were provided by the Tissue Bank of the National Center for Tumor Diseases (NCT, Heidelberg, Germany) in accordance with the ethics committee of the University of Heidelberg. J. Vockley was funded in part by PHS grant NIH R01-DK78775. Part of the work was funded by a grant of the DFG to B.K. Straub (STR 1160/1-2). This study was

supported by the German Bundesministerium für Bildung und Forschung (BMBF) through the German Network for mitochondrial disorders (mitoNET, 01GM1113C to T.M. and H.P.) and through the E-Rare project GENOMIT (01GM1207 for T.M. and H.P.). T.B.H. was supported by the BMBF through the Juniorverbund in der Systemmedizin "mitOmics" (FKZ 01ZX1405C).

#### Compliance with Ethical Standards

#### Conflict of Interest None.

**Informed Consent** All procedures followed were in accordance with the ethical standards of the responsible committee on human experimentation (institutional and national) and with the Helsinki Declaration of 1975, as revised in 2000.

#### References

- Aoki T, Ichimura S, Itoh A et al (2009) Identification of the neuroblastoma-amplified gene product as a component of the syntaxin 18 complex implicated in Golgi-to-endoplasmic reticulum retrograde transport. Mol Biol Cell 20(11):2639–2649
- Boyadjiev SA, Fromme JC, Ben J et al (2006) Cranio-lenticulo-sutural dysplasia is caused by a SEC23A mutation leading to abnormal endoplasmic-reticulum-to-Golgi trafficking. Nat Genet 38(10): 1192–1197
- Garcia Segarra N, Ballhausen D, Crawford H et al (2015) NBAS mutations cause a multisystem disorder involving bone, connective tissue, liver, immune system, and retina. Am J Med Genet Part A 9999A:1–11
- Haack TB, Hogarth P, Kruer MC et al (2012) Exome sequencing reveals de novo WDR45 mutations causing a phenotypically distinct, X-linked dominant form of NBIA. Am J Hum Genet 91(6):1144–1149
- Haack TB, Staufner C, Kopke MG et al (2015) Biallelic mutations in NBAS cause recurrent acute liver failure with onset in infancy. Am J Hum Genet 97(1):163–169
- He M, Rutledge SL, Kelly DR et al (2007) A new genetic disorder in mitochondrial fatty acid beta-oxidation: ACAD9 deficiency. Am J Hum Genet 81(1):87–103
- Jones B, Jones EL, Bonney SA et al (2003) Mutations in a Sar1 GTPase of COPII vesicles are associated with lipid absorption disorders. Nat Genet 34(1):29–31
- Kim SU, Choi GH, Han WK et al (2010) What are 'true normal' liver stiffness values using FibroScan?: a prospective study in healthy living liver and kidney donors in South Korea. Liver Int: Off J Int Assoc Study Liver 30(2):268–274
- Longman D, Hug N, Keith M et al (2013) DHX34 and NBAS form part of an autoregulatory NMD circuit that regulates endogenous RNA targets in human cells, zebrafish and Caenorhabditis elegans. Nucleic Acids Res 41(17):8319–8331
- Lossie AC, Muir WM, Lo CL et al (2014) Implications of genomic signatures in the differential vulnerability to fetal alcohol exposure in C57BL/6 and DBA/2 mice. Front Genet 5:173
- Lubbehusen J, Thiel C, Rind N et al (2010) Fatal outcome due to deficiency of subunit 6 of the conserved oligomeric Golgi complex leading to a new type of congenital disorders of glycosylation. Hum Mol Genet 19(18):3623–3633
- Maksimova N, Hara K, Nikolaeva I et al (2010) Neuroblastoma amplified sequence gene is associated with a novel short stature syndrome characterised by optic nerve atrophy and Pelger-Huet anomaly. J Med Genet 47(8):538–548



- Narkewicz MR, Dell Olio D, Karpen SJ et al (2009) Pattern of diagnostic evaluation for the causes of pediatric acute liver failure: an opportunity for quality improvement. J Pediatr 155(6):801–806, e801
- Pawella LM, Hashani M, Eiteneuer E et al (2014) Perilipin discerns chronic from acute hepatocellular steatosis. J Hepatol 60(3):633–642
- Squires RH Jr, Shneider BL, Bucuvalas J et al (2006) Acute liver failure in children: the first 348 patients in the pediatric acute liver failure study group. J Pediatr 148(5):652–658
- Straub BK, Stoeffel P, Heid H, Zimbelmann R, Schirmacher P (2008)
  Differential pattern of lipid droplet-associated proteins and de novo
- perilipin expression in hepatocyte steatogenesis. Hepatology 47(6): 1936–1946
- Uemura T, Sato T, Aoki T et al (2009) p31 deficiency influences endoplasmic reticulum tubular morphology and cell survival. Mol Cell Biol 29(7):1869–1881
- Vilarinho S, Choi M, Jain D et al (2014) Individual exome analysis in diagnosis and management of paediatric liver failure of indeterminate aetiology. J Hepatol 61(5):1056–1063
- Ward CL, Omura S, Kopito RR (1995) Degradation of CFTR by the ubiquitin-proteasome pathway. Cell 83(1):121–127

